

1995/19494

1.
APPENDIX C-1

N95-25914

A Study of the Radiation Environment On Board the Space Shuttle Flight STS-57

53-72
44027
p. 24

G.D. Badhwar, W. Atwell*, E.V. Benton*, A.L. Frank* and R.P. Keegan*

NASA Johnson Space Center, Houston, Texas 77058

Rockwell, Space Systems Division, Houston, Texas 77058

Department of Physics, University of San Francisco, San Francisco, CA 94117-1080

and

V.E. Dudkin, O.N. Karpov, Yu. V. Potapov, A.B. Akopova

Research Center for Spacecraft Radiation Safety

Shchukinskaya Str. 40, Moscow 123182, Russia

and

N.V. Magradze, L.V. Melkumyan, and Sh. B. Rshtuni

Yerevan Physics Institute, Yerevan 375036, Armenia



Abstract

A joint NASA-Russian study of the radiation environment inside a SPACEHAB 2 locker on Space Shuttle flight STS-57 was conducted. The Shuttle flew in a nearly circular orbit of 28.5° inclination and 462 km altitude. The locker carried a charged particle spectrometer, a tissue equivalent proportional counter (TEPC), and two area passive detectors consisting of combined NASA plastic nuclear track detectors (PNTDs) and thermoluminescent detectors (TLDs), and Russian nuclear emulsions, PNTDs and TLDs. All the detector systems were shielded by the same Shuttle mass distribution. This makes possible a direct comparison of the various dose measurement techniques. In addition, measurements of the neutron energy spectrum were made using the proton recoil technique.

The results show good agreement between the integral LET spectrum of the combined galactic and trapped particles using the tissue equivalent proportional counter and track detectors between about 15 keV/μm and 200 keV/μm. The LET spectrum determined from nuclear emulsions was systematically lower by about 50%, possibly due to emulsion fading. The results show that the TEPC measured an absorbed dose 20% higher than TLDs, due primarily to an increased TEPC response to neutrons and a low sensitivity of TLDs to high LET particles under normal processing techniques. There is a significant flux of high energy neutrons that is currently not taken into consideration in dose equivalent calculations. The results of the analysis of the spectrometer data will be reported separately.

Introduction

The complex radiation environment in low-Earth orbits has received considerable attention for the past three decades. Detailed knowledge of this environment under varied spacecraft shielding geometry is necessary for minimizing risk due to radiation exposure. The radiation exposure received by crew members in space flights has primarily been studied using passive thermoluminescent detectors (TLDs). Although some measurements of the linear energy transfer spectrum have been made using plastic nuclear track detectors (PNTDs) and nuclear emulsions, they have rarely been used in assessing crew exposures. Active ionization chambers have flown on the Skylab mission (Parnell et al., 1986) and are currently used on the Mir orbital station. Although ionization chambers provide dose rate data, they do not provide the LET spectrum which is the key to obtaining effective dose equivalent. High energy (≥ 0.5 MeV) neutron measurements have received virtually no attention in the US space program. Active tissue equivalent proportional counters have been flown on a limited number of Shuttle flights. The Radiation Monitor Equipment (RME) is a three channel detector that provides absorbed dose, and a rough estimate of dose equivalent as a function of mission elapsed time (Golightly et al., 1994). Badhwar et al. (1992, 1994a) have flown, first, a 15-channel and more recently, a 512-channel tissue equivalent counter in a number of Shuttle flights. Nguyen et al. (1989) flew a dose and dose-equivalent meter on the Mir station, and now a new instrument that provides the LET spectrum is onboard the Mir station. These measurements indicate that estimates of radiation exposure using passive TLDs are low compared to those measured using active

detectors. The PNTDs do not respond to radiation below about 5 keV/ μm , a region that can contribute nearly 60-70% of the absorbed dose. These detectors are not fully efficient till about 10-15 keV/ μm . The nuclear track detectors, because of their simplicity, have been routinely flown on virtually all Shuttle flights. However, a direct comparison of these measurements with active detectors has not been possible, because invariably the active and passive detectors were flown under different Shuttle mass shielding. This current experiment was designed to remedy these problems.

This paper describes the results of absorbed dose, dose equivalent, LET spectrum, and neutron energy spectrum inside a Shuttle locker.

Experimental Details

The flight experiment consisted of four separate detector systems: (i) a charged particle directional spectrometer (CPDS), (ii) a tissue equivalent proportional counter (TEPC), (iii) two area passive detectors with combined NASA and Russian complements. All four of these detectors were housed inside a SPACEHAB 2 locker. The SPACEHAB 2 itself was in the payload bay of the Space Shuttle. Thus all of the detectors saw nearly identical mass shielding distribution.

Figure 1 is a schematic of the particle spectrometer. It consists of two 1 mm thick lithium drifted silicon detectors, A1 and A2, that define the basic telescope geometry. At the top

of each of these detectors are 16 x 16 strip detectors to determine the x,y coordinates of those particles that formed the coincidence A1A2. Each of these silicon position-sensitive detectors (PSDs) is 300 μm thick. This basic telescope was followed by six 5 mm thick lithium drifted silicon detectors, B1 to B6, followed by a 1 mm thick A3, PSD 3, and 1 cm thick sapphire Cerenkov detector viewed head-on by a photomultiplier tube. The area-solid product of the A1A2 coincidence is 6.2 $\text{cm}^2 \text{ sr}$ for an isotropic incidence flux. For A1A2 coincidences, the voltage output of every detector is pulse-height analyzed using 4096 channel analog-to-digital converters.

The tissue equivalent proportional counter (Figure 2) consists of a cylindrical detector 1.78 cm long and 1.78 cm in diameter simulating a $\sim 2 \mu\text{m}$ -diameter site that is bounded by tissue-equivalent plastic. The detector uses low pressure gas and operates around -750 volts. The detector signal is processed by a very low-noise preamplifier and two amplifiers that differ in gain by a factor of 50. The pulse height of the voltage output from each amplifier is analyzed in a 256-channel analog-to-digital converter. The root mean square of the electronic system noise is approximately 130 electrons at room temperature. The lower level discriminator is set around 0.2 $\text{keV}/\mu\text{m}$. The instrument covers a lineal energy range, y , from about 0.2 to 1250 $\text{keV}/\mu\text{m}$. The energy resolution of the electronics is 0.1 $\text{keV}/\mu\text{m}$ below 20 $\text{keV}/\mu\text{m}$ and 5 $\text{keV}/\mu\text{m}$ above 20 $\text{keV}/\mu\text{m}$. The full lineal energy spectrum is recorded every minute. In addition, absorbed dose is computed by the instrument and recorded either every 2 or 20 s depending upon the dose rate.

The proportional counter was calibrated in terms of lineal energy by exposing it to fission neutrons and ^{137}Cs sources. The detector calibration was verified post flight by using 80 and 170 MeV protons at the University of Loma Linda, California, proton accelerator.

The NASA portions of the area passive detectors contained TLD-700, CR-39, TLD-600 with CR-39 and Gd foils to measure thermal and epi-thermal neutrons. The Russian portions contained TLD-600, CR-39, and Soviet Bya- and BR-type nuclear photo-emulsions.

The STS-57 flight was launched in to $28.5^\circ \times 462$ km nearly circular orbit on June 21, 1993 for a period of 9.986 days. The TEPC and CPDS were turned on after attaining orbit and turned off prior to re-entry.

Data Analysis

The methods of analysis of data from these detectors is unique to each detector system. These methods are discussed separately in previous publications. The analysis of the spectrometer data followed the procedure described in Badhwar et al. (1994b), is not yet completed, and will be reported separately. Figure 3 shows the A1 counting rate and A1A2 coincidence rate as a function of mission elapsed time. The large spikes are the Shuttle passes through the South Atlantic Anomaly (SAA). A1 and A2 are thin planar detectors and count particles coming from any direction. The coincidence rate A1A2

restricts the opening to particles within a cone of 45° full angle. Because of the anisotropic nature of trapped particle flux and the viewing angle, the A1A2 count rate shows a different time profile than the omni-directional detector A1. Particles that form the A1A2 coincidence provide a measure of the average energy loss per particle. This can be determined separately for trapped and galactic particle portions of the Shuttle orbit. Thus individual A1 or A2 count rate can appropriately be scaled to dose rates in silicon.

Figure 3 plots the TEPC measured dose rate as a function of the mission elapsed time. This information has been used to separate the data into categories of trapped (SAA) and galactic cosmic rays (GCR). The method of analysing TEPC data has been described in detail (Badhwar et al., 1994a).

The analysis of the NASA TLDs and CR-39 followed well established techniques that are described in a number of publications from Benton et al. (1983a,b, 1988, 1991) and Csige et al. (1991). The techniques for determining the LET spectrum from nuclear emulsions are described by Akopova et al., (1985, 1987, 1990). The differentail fast-neutron energy spectrum was measured using the recoil proton energy spectrum generated as a result of the elastic scattrng of neutrons from unbounded hydrogen in the emulsions.

Measurements were made only of proton tracks whose ends were located within the volume of the emulsion. Due to a significant visual inefficiency of the short path-length recoil protons ($E_n \leq 1$ MeV) and proton contamination from $^{14}\text{N}(n,p)$ reaction with emulsion nitrogen, neutron fluxes with $E_n < 1$ MeV were not measured. More detailed

description of this technique can be found in Dudkin et al. (1990). We refer the reader to these publications for more details.

Results

Dose Measurements

The dose rate measured using the tissue equivalent proportional counter was 1109.7 $\mu\text{Gy}/\text{day}$, with GCR particles contributing 71.3 $\mu\text{Gy}/\text{day}$ and trapped particles contributing 1038.4 $\mu\text{Gy}/\text{day}$. The TLDs mounted on the front surface of the APD box measured 929 ± 28 and 936 ± 28 μGy and those mounted on the back surface measured 920 ± 28 and 909 ± 27 μGy . The average dose rate using TLDs was 925.3 $\mu\text{Gy}/\text{day}$. The dose rate measured by TEPC is 20% higher than this rate. The reason for this difference is that the TEPC responds to neutrons whereas the TLDs do not under normal processing. Also, TLDs are less sensitive to high LET particles.

Neutron Spectrum

The fast-neutron spectrum was calculated using the measured recoil proton energy spectrum generated as a result of the elastic (n,p) scattering of neutrons from the hydrogen in the emulsion. Figure 4 shows the derived spectrum in $\sim 1\text{-}15$ MeV range. Integrating this spectrum gives an absorbed dose rate of 20 $\mu\text{Gy}/\text{day}$ and dose equivalent

rate of 174 $\mu\text{Sv/day}$. This dose equivalent is a factor of nearly 3 higher than in STS-55 (6 $\mu\text{Gy/day}$ and 53 $\mu\text{Sv/day}$) derived using the same technique (Dudkin et al., 1994) and factor 4 to 8 higher than in high inclination COSMOS flights that missed the SAA (Dudkin et al., 1990). The STS-57 flight was in a higher 462 km altitude orbit compared to STS-55 (28.5° x 290 km). These results suggest that a large fraction of the neutrons are produced in the Shuttle shielding by the interactions of trapped protons and GCR. This is quite consistent with observations of Keith et al. (1992) that indicated that at Dloc 2 location in the Shuttle mid-deck nearly 80% of the neutrons below 15 MeV were due to secondaries and 20% were due to atmospheric albedo. Based on a number of thermal and epi-thermal neutron measurements (< 1 MeV) under the same shielding, Benton et al. (1988) have estimated their dose equivalent contribution of less than 1 MeV neutrons to be about 22 $\mu\text{Sv/day}$. Thus we have about a 200 $\mu\text{Sv/day}$ contribution to dose equivalent from thermal to about 15 MeV. Model calculations (Armstrong and Colburn, 1992, Keith et al., 1992) suggest that this energy region provides only about one-half of the total dose equivalent. Thus the dose equivalent contributions from neutrons could approach nearly 400 $\mu\text{Sv/day}$ on this flight, which is higher than the dose contributed by the GCR particles. It is important to note that the depth-dose equivalent of neutrons in body tissue is markedly different than that of protons. At organ levels then, neutrons could provide a much higher dose equivalent than GCR particles at the STS-57 (or higher) altitudes.

Linear Energy Transfer Spectra

Figure 5 is the integral LET spectrum of the combined trapped and galactic particles. The spectrum measured by the CR-39 PNTDs, incorporating a technique that enhances the efficiency of very high LET events, is shown for comparison. THE PNTD measurements fall somewhat above TEPC at high LETs (by approximately a factor of 2), then gradually merge with TEPC data at about 15-50 keV/ μm and fall below at low LETs. This difference may be due in part to the short range secondaries produced in the two detectors. The lining of the TEPC sensitive volume is tissue-equivalent, while the CR-39 PNTD is $\text{O}_7\text{C}_{12}\text{H}_{18}$. The CR-39 therefore has a higher density of heavier nuclei and lower density of hydrogen, as compared to TEPC liner. Secondary particle spectra produced by primaries interacting with nuclei in the two media will therefore be different. A greater fluence of high LET secondaries would be expected in the CR-39 while a greater fluence of light, proton recoil (low LET) secondaries would be expected in the TEPC, in qualitative agreement. In addition, the CR-39 loses efficiency below ~ 15 keV/ μm which explains the fall-off below TEPC measurements in the low LET region. The solid circles are data obtained using the nuclear emulsion technique. The shape of this spectrum above ~ 10 keV/ μm is nearly the same as the TEPC spectrum, but it is systematically lower in flux by about a factor of 2.3. The charged particle flux at this altitude is dominated by the anisotropic trapped particles. The area-solid angle product however has been calculated using the assumption of an isotropic flux. This can lead to a systematic increase in the calculated flux. Nuclear emulsions from this flight could not be immediately returned to Moscow. The delay could have lead to fading and hence a lower efficiency. A combination of these two effects is the probable cause of the lower flux. The average quality factors

using the ICRP-60 definition, were 1.86 for the whole flight, 3.08 for galactic cosmic rays and 1.78 for trapped particles. Thus GCR particles contribute 220 $\mu\text{Sv/day}$, which is nearly equal to the contribution from neutrons with energies between thermal and ~ 15 MeV.

Thus, under moderate shielding thicknesses the neutron contribution to dose and dose equivalent cannot be ignored. This is roughly 20% of the charged particle skin dose equivalent and about twice what was observed using Bonner spheres and gold activation foil techniques in earlier Shuttle flights, including the highest altitude flight to date, the STS-31 Hubble mission (Keith et al., 1992). However, for these measurements the Bonner spheres were mounted in one of the least shielded locations (Dloc 2) in the mid-deck. Skin doses received by astronauts are more typical of a higher shielding than this location. Clearly, additional neutron measurements are essential to quantify the neutron dose contribution for long duration flights.

Figure 6 and 7 show the integral LET spectra of trapped and GCR particles separately. The solid lines are model calculations based on the AP-8 Min (Sawyer and Vette, 1976) and the GCR model of Badhwar and O'Neill (1994). It was shown earlier that the absorbed dose calculated using the AP-8 Min model is a factor of 1.8 higher than the measured absorbed dose. Thus the AP-8 model calculated spectrum was normalized by this factor. There is reasonable agreement in the shape of the measured and model spectra in the intermediate LET range about 15 to 100 keV/ μm , however, this is not the case at

both low and high LET ends. The particle spectrometer has confirmed the presence of less than 6 MeV secondary electrons. These electrons would be seen by the proportional counter but not by the CR-39 or nuclear emulsion. These electrons are not taken in to account in the model either. The GCR radiation transport calculations were done using the recently modified HZETRN code (Cucinotta, 1993, 1994). There is very good agreement between the model calculations and observations, except at very high LETs.

Conclusions

A joint NASA-Russian experiment was flown on the SPACEHAB 2 mission in 28.5° x 462 km orbit. This altitude is very close to that of the planned International Space Station Alpha, which will be in a 51.8° inclination orbit and will thus see more galactic cosmic radiation flux than in this flight. The results have shown that: (i) there is good agreement between the TEPC and PNTD measured LET spectra from about 15 keV/μm to 200 keV/μm, (ii) the shape of the nuclear emulsion deduced spectrum is the same as that determined from these two techniques, (iii) the total absorbed dose measured using TEPC is 20% higher than the total dose measured using TLDs, (iv) there is a substantial flux of high energy neutrons that contribute at least as much dose equivalent as the galactic particles, and more likely nearly twice as much, and (v) these neutrons are essentially all secondaries generated by the interactions of trapped and galactic particles with spacecraft shielding. This implies that there is a significant secondary proton component also. This neutron contribution must be taken into account for crew risk assessment, particularly for long duration missions at higher than 400 km altitudes.

Acknowledgments

This experiment was started with remarkable support and encouragement of Mr. Timothy White, Assistant to the Director of Space and Life Sciences, Johnson Space Center, Houston, Texas and built and flight certified in near record time of one year. Mr. Dennis

Grounds and Dr. Dane Russo provided excellent support and encouragement. Mr. Terry Byers and Ken Kaufman provided excellent flight integration support. We appreciate the excellent programming support of Mr. Omar Baltaji and Fadi Riman, and mechanical engineering support of Mr. Robert Dunn, all of Lockheed. Dr. Thomas Conroy, Battelle Pacific Northwest Laboratory, Richland, WA, provided electronic engineering support. Frank Gibbons and Terry Byers were instrumental in getting the position sensitive detectors to work. We are grateful for the hard work of all these individuals. We are also grateful to Luis Frigo and El-Sayed Awad for important contributions with regard to the PNTD data. The University of San Francisco portion of the work was supported by NASA grants Nos. NAG9-235 and NAGW-4154.

References

Akopova, A.B., Dudkin V.E., Kovalev E.E., Magradze N.V., and Potapov Yu. V. (1987) Linear energy transfer spectra of cosmic radiation aboard Cosmos-1129 artificial; satellite. *Radiat. Prot. Dosim.* **18**, 153-156.

Akopova, A.B., Magradze N.V., Dudkin V.E., Kovalev E.E., Potapov Yu. V., Benton E.V., Frank A.L., Benton E.R., Parnell T.A. and Watts J.W. Jr. (1990) Linear energy transfer (LET) spectra of cosmic radiation in low Earth orbit. *Nucl. Tracks Radiat. Meas.* **17**, 93-97.

Akopova, A.B., Vikhrov A.I., Dudkin V.E., Magradze N.V., Moiseenko A.A., Muradyan A.H., Ovnanyan K.M. and Potapov Yu. V. (1985) Measuring the linear energy transfer spectra of cosmic radiation aboard the Cosmos-1129 satellite. *Kosm. Issled XXIII*, 479-481.

Armstrong, T.W., and Colborn B.L. (1992) Predictions of induced radioactivity for spacecraft in low Earth orbit, *Nucl. Tracks Radiat. Meas.*, **20**, 101-130.

Badhwar, G.D., Konradi A., Hardy A., and Braby L.A (1992) Active dosimetric measurements on Shuttle flights, *Nucl. Tracks Radiat. Meas.* **20**, 13-20.

Badhwar, G.D., Cucinotta F.A., Braby L.A., and Konradi A., Measurements on the Shuttle of the LET spectra of galactic cosmic radiation and comparison with radiation transport model, *Radia. Res.* **139**, 344-351.

Badhwar, G.D., Patel J.U., Cucinotta F.A., and Wilson J.W. (1994) Measurements of the secondary particle energy spectra in the space Shuttle, *Radiat. Meas.* (to be published).

Badhwar, G.D., and O'Neill P.M. (1993), Time lag of twenty two year solar modulation. In Proceedings of the *23rd International Cosmic Ray Conference*, **3**, 535-539, Calgary.

Benton, E.V. (1983) Dosimetric radiation measurements in space. *Nucl. Tracks Radiat. Meas.* **7**, 1-11.

Benton, E.V. and Henke R.P. (1983) Radiation exposures during space flight and their measurements. *Adv. Space Res.* **3**, 171-185.

Benton, E.V. and Parnell, T.A. (1988) Space radiation dosimetry on U.S. and Soviet Manned missions, in NATO ASI Series A, Life Sciences, **154**, *Terrestrial Space Radiation and its Biological Effects*, P.D. McCormack, C.E. Swenburg and H. Bucker, eds. Plenum Press (1988), pp729-794.

Benton, E.V., Frank, A.L., Benton, E.R., Csige, I., Parnell, T.A., and Watts, J.W. Jr. (1991), Radiation exposure of LDEF: Initial results, Proceedings of *LDEF: 69 Months in Space*, Kissimmee, Florida, June 2-8, 1991.

Csige, I., Benton, E.V., Frank, A.L., Figo, L.A., Benton, E.R., Parnell, T.A., and Watts, J.W. Jr. (1991), Charged particle LET spectra measurements aboard LDEF, Proceedings of *LDEF: 69 Months in Space*, Kissimmee, Florida, June 3-8, 1991

Cucinotta, F.A. (1993) Calculations of cosmic ray helium transport in shielding materials, TP 3354, NASA, Washington, DC, also private communication September 1994.

Dudkin, V.E., Potapov Yu. V., Akova A.B., Melkumyan L.V., E.V. Benton, and Frank A.L. (1990) Differential neutron energy spectra measured on spacecraft in low earth orbit. *Nucl. Tracks Radiat. Meas.* 17, 87-91.

Dudkin, V.E., Karpov O.N., Potapov Yu. V., Akopova A.B., Magradze N.V., Melkumyan L.V., and Rshtuni Sh. B. (1994) Study of the radiation environment on board STS-55 and STS-57 by passive detectors method, In Proceedings of *12th International Conference on Nuclear Tracks in Solids*, Dubna, Russia, August 24-28.

Golightly, M.J., Hardy K., and Quam W. (1994) Radiation dosimetry measurements during U.S. Space Shuttle missions with the RME-III, *Radiat. Meas.* 23, 25-42.

Keith, J.E., Badhwar G.D., and Lingstrom D.J. (1992) Neutron spectrum and dose-equivalent in shuttle flights during solar maximum, *Nucl. Tracks Radiat. Meas.* 20, 41-48.

Nguyen, V.D., Bouisset P., Parmentier N., et al. (1989) Real time quality factor and dose equivalent meter "CIRCE" and its use on board the Soviet orbital station MIR. In *Humans in Earth Orbit and Planetary Exploration Missions, Int. Acad. Astronaut. 8th Symp.* Tashkent, Uzbekistan, U.S.S.R

Parnell, T.A., Watts J.W. Jr., Fishman G.J., Benton E.V., Frank A.L., and Gregory J.C. (1986) The measured radiation environment within Spacelab 1 and 2 and comparisons with predictions, *Adv. Space Res.*, 6, 125-137.

Sawyer, D.M. and Vette J.I. (1976) AP-8 trapped proton environment for solar maximum and minimum. Report NSSDC/WDC-A-R&S 76-06, NASA, Goddard Space Flight Center, Greenbelt, Maryland

Figure Captions

Figure 1: A schematic diagram of the charged particle telescope

Figure 2: A schematic diagram of the tissue equivalent proportional counter

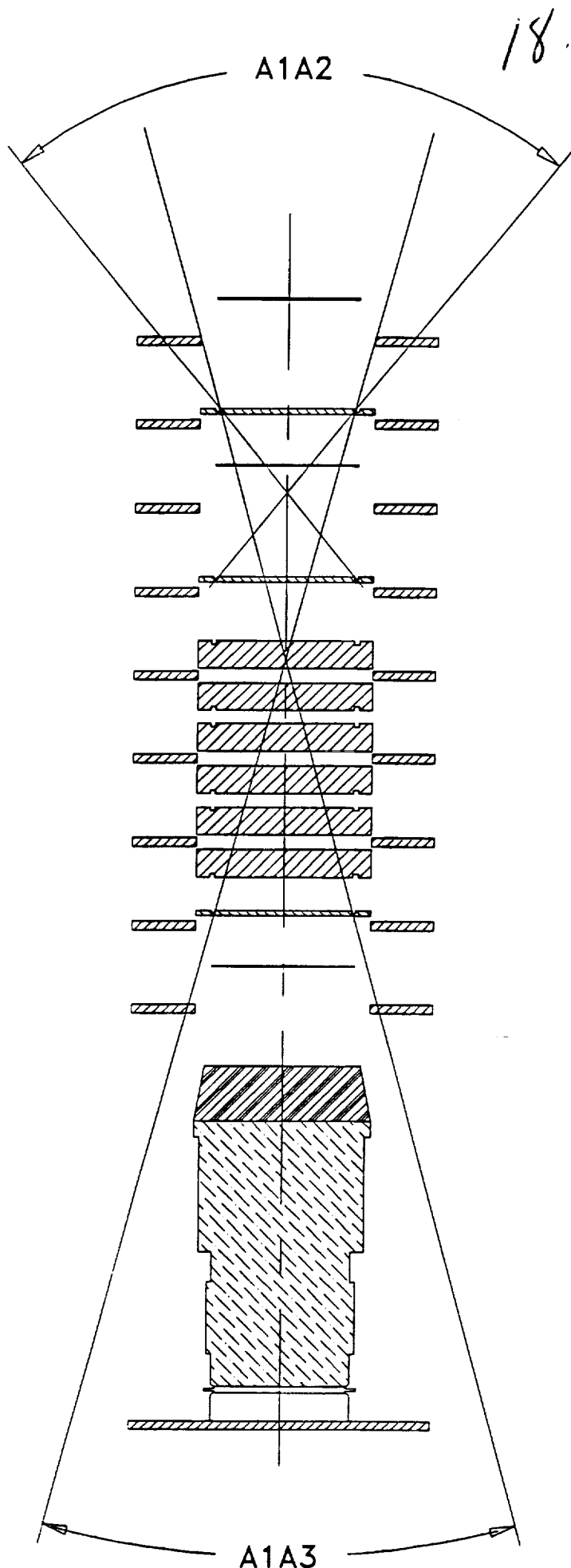
Figure 3: Plots of the TEPC measured dose rate, A1 single and A1A2 coincidence rate as a function of the mission elapsed time.

Figure 4: Plot of the neutron energy spectrum measured using proton recoil technique.

Figure 5: Plot of the integral linear energy transfer spectrum using TEPC, CR-39, and nuclear emulsions.

Figure 6: Plot of the trapped particle integral LET spectrum and comparison with model calculations.

Figure 7: Plot of the GCR integral LET spectrum and comparison with model calculations.



18.

PSD 1 [25x25x0.003mm]

A1 [φ25x1mm]

PSD 2 [25x25x0.003mm]

A2 [φ25x1mm]

B1 [φ25x5mm]

B2 [φ25x5mm]

B3 [φ25x5mm]

B4 [φ25x5mm]

B5 [φ25x5mm]

B6 [φ25x5mm]

A3 [φ25x1mm]

PSD 3 [25x25x0.003mm]

CERENKOV

C DET

FIG 1

19.

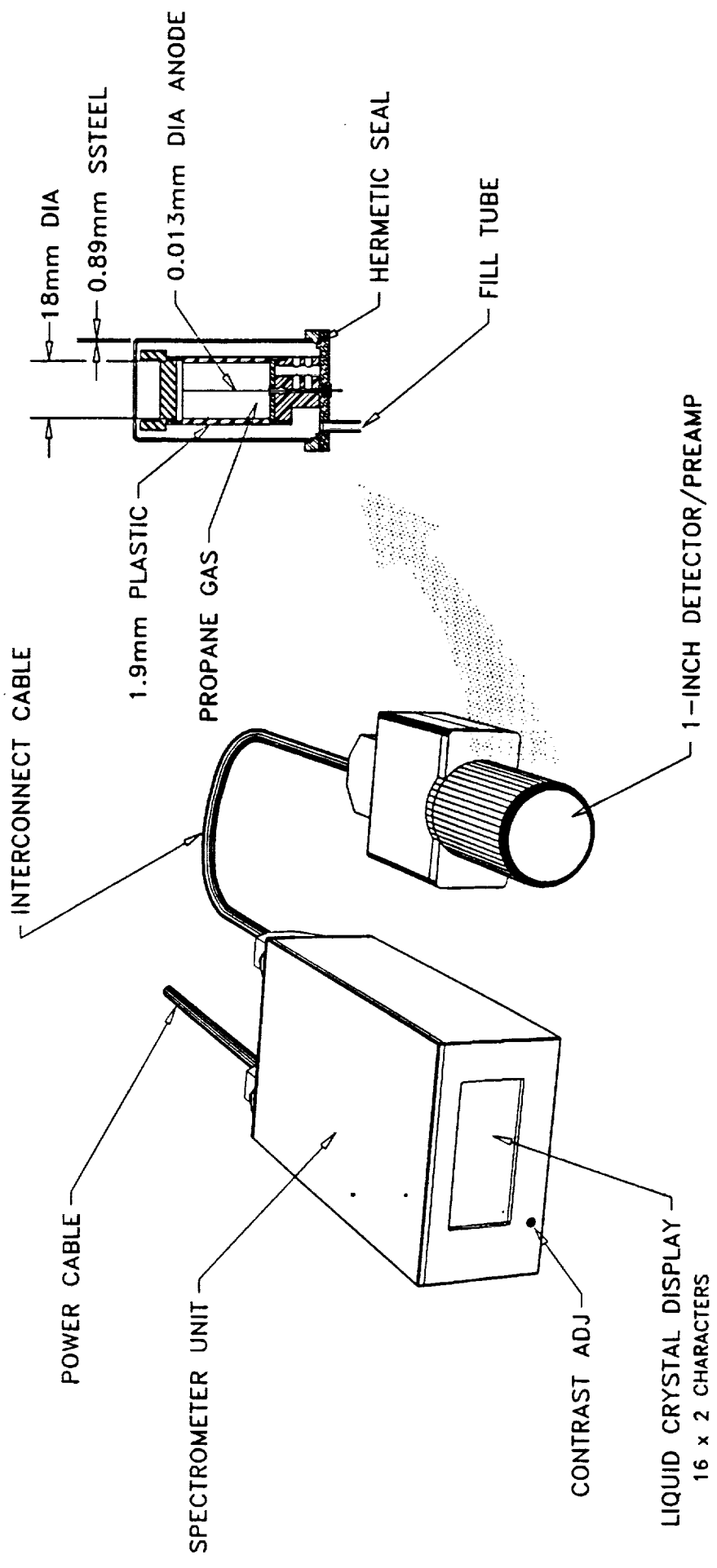


FIG. 2

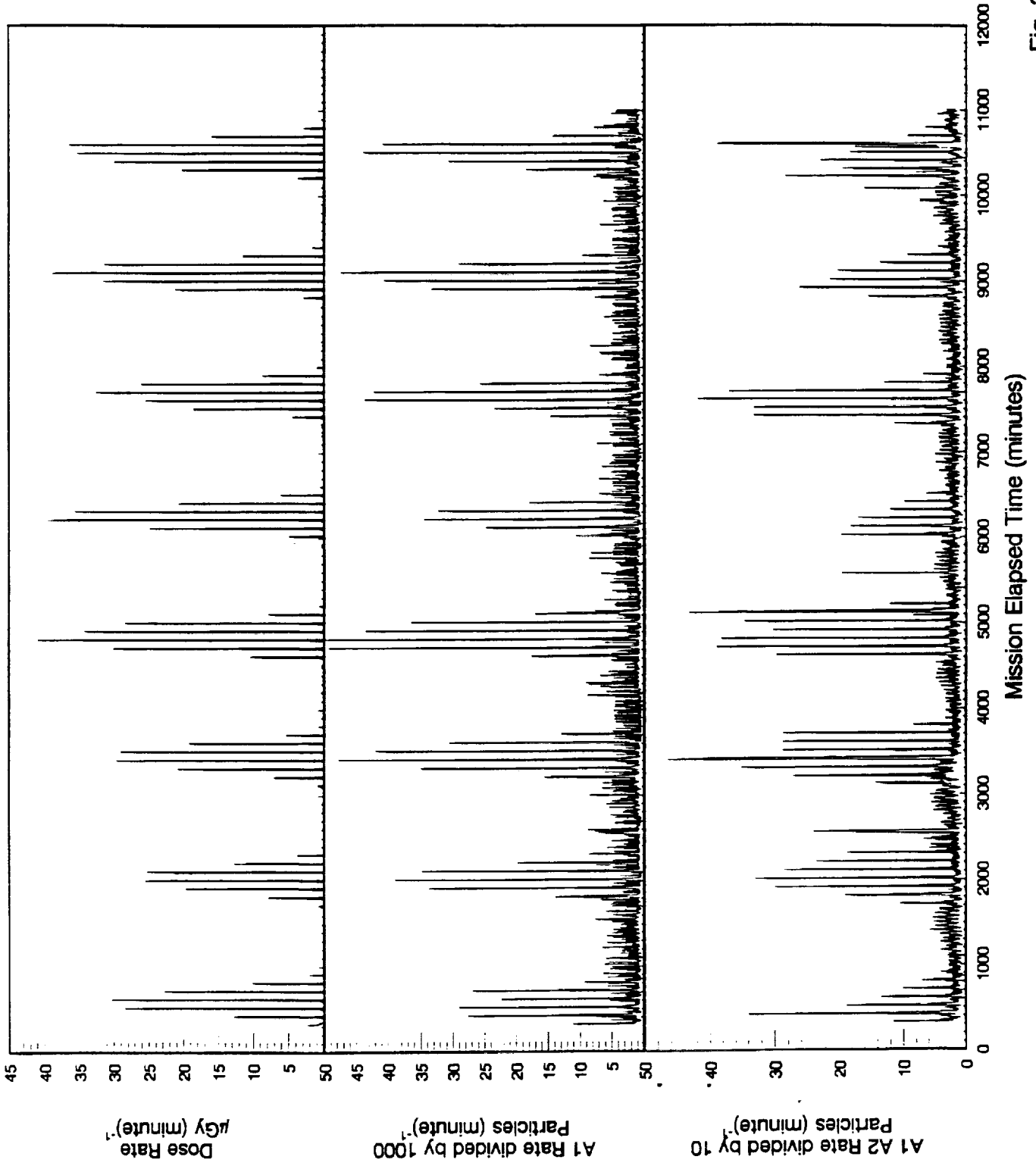


Fig. 3

50.

21.

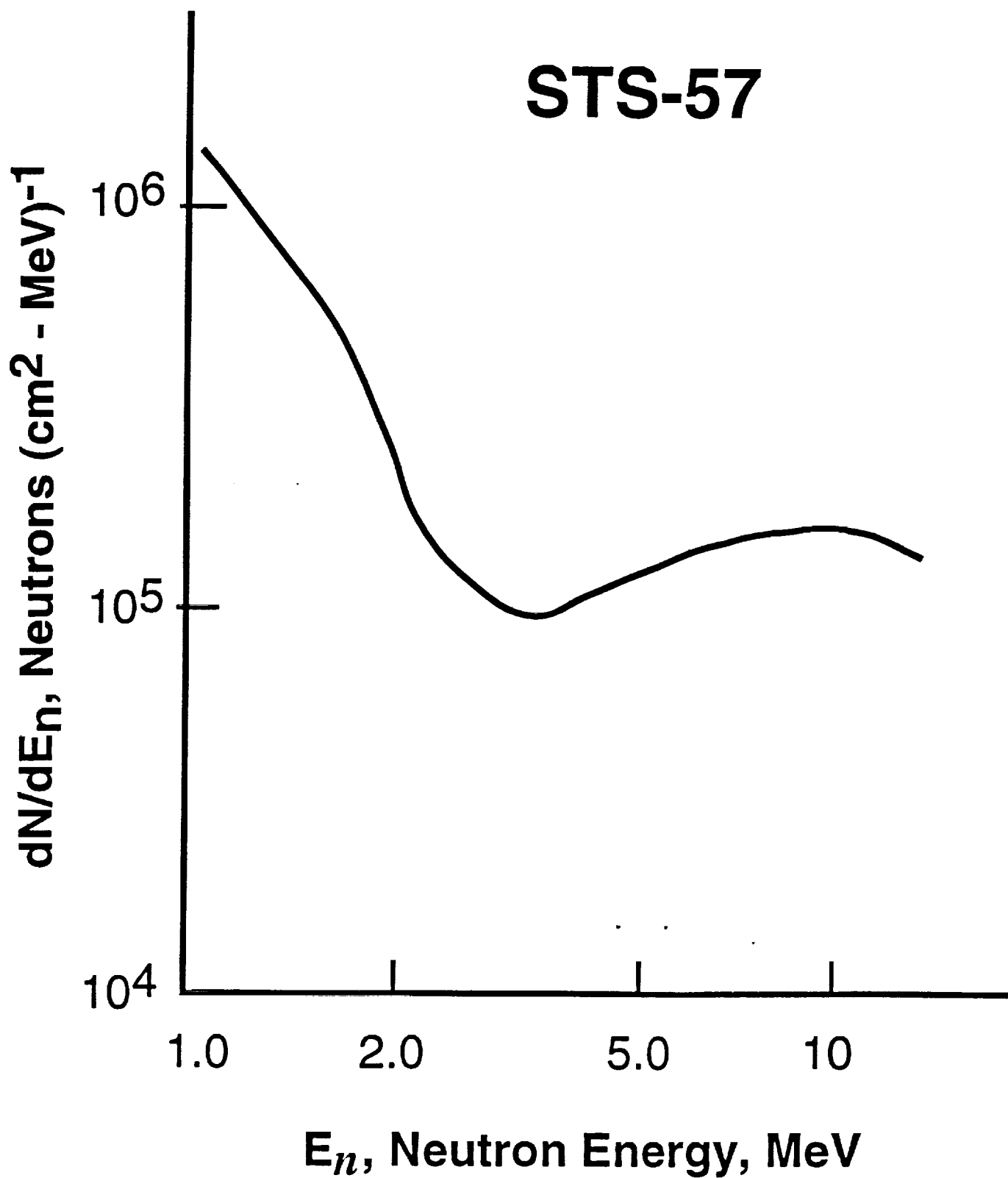


FIG. 4

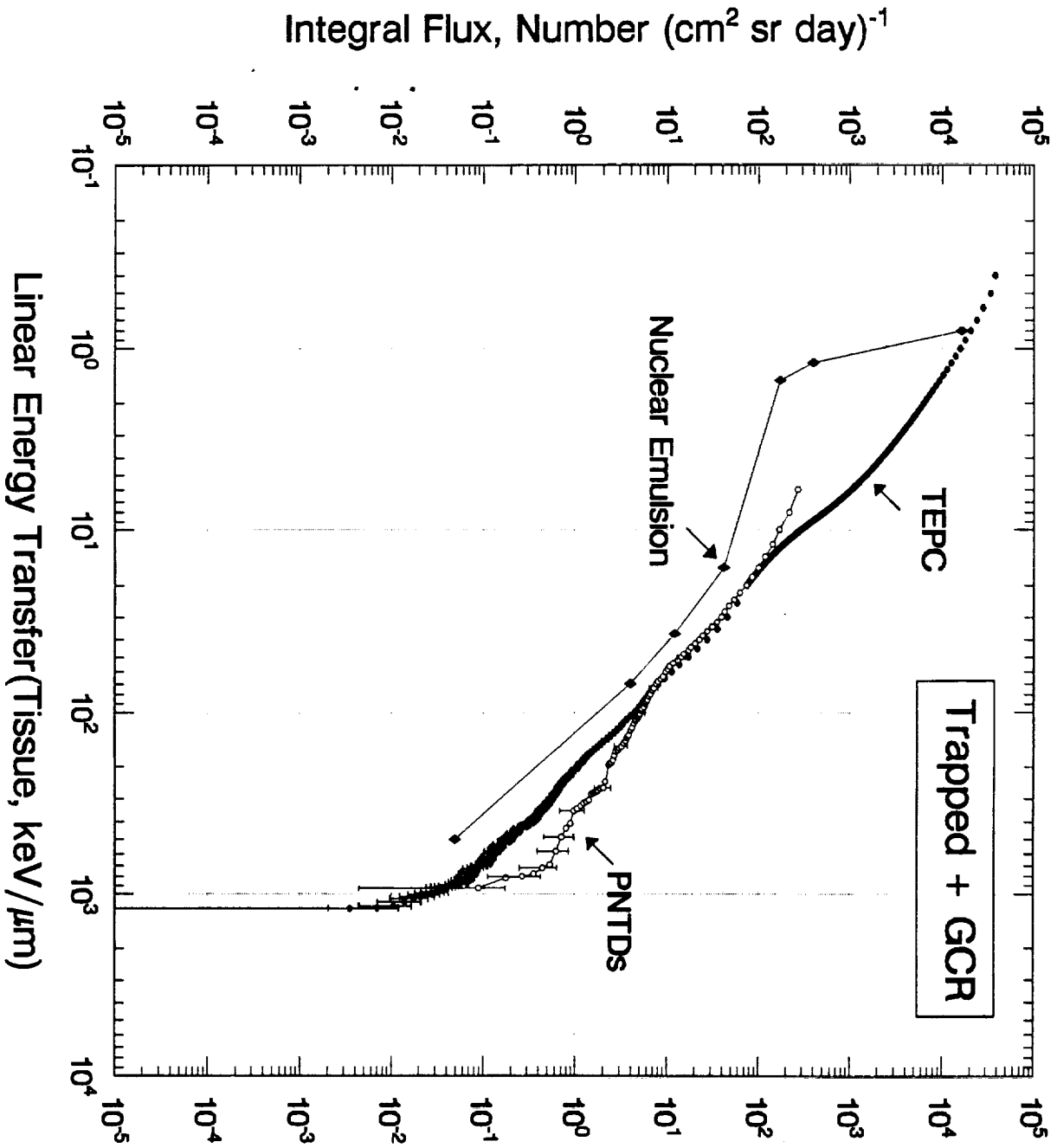


Fig. 5

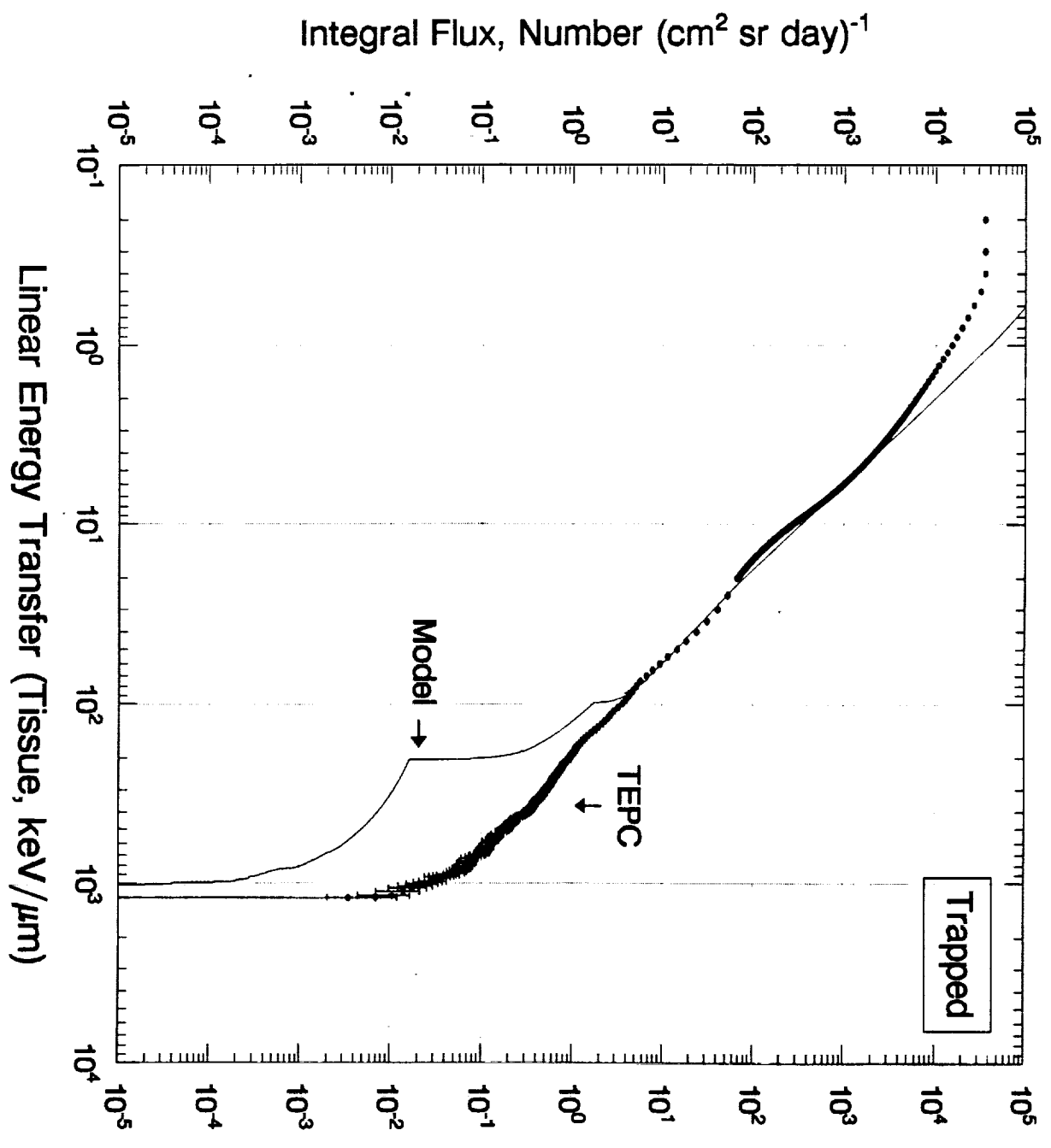


Fig. 6

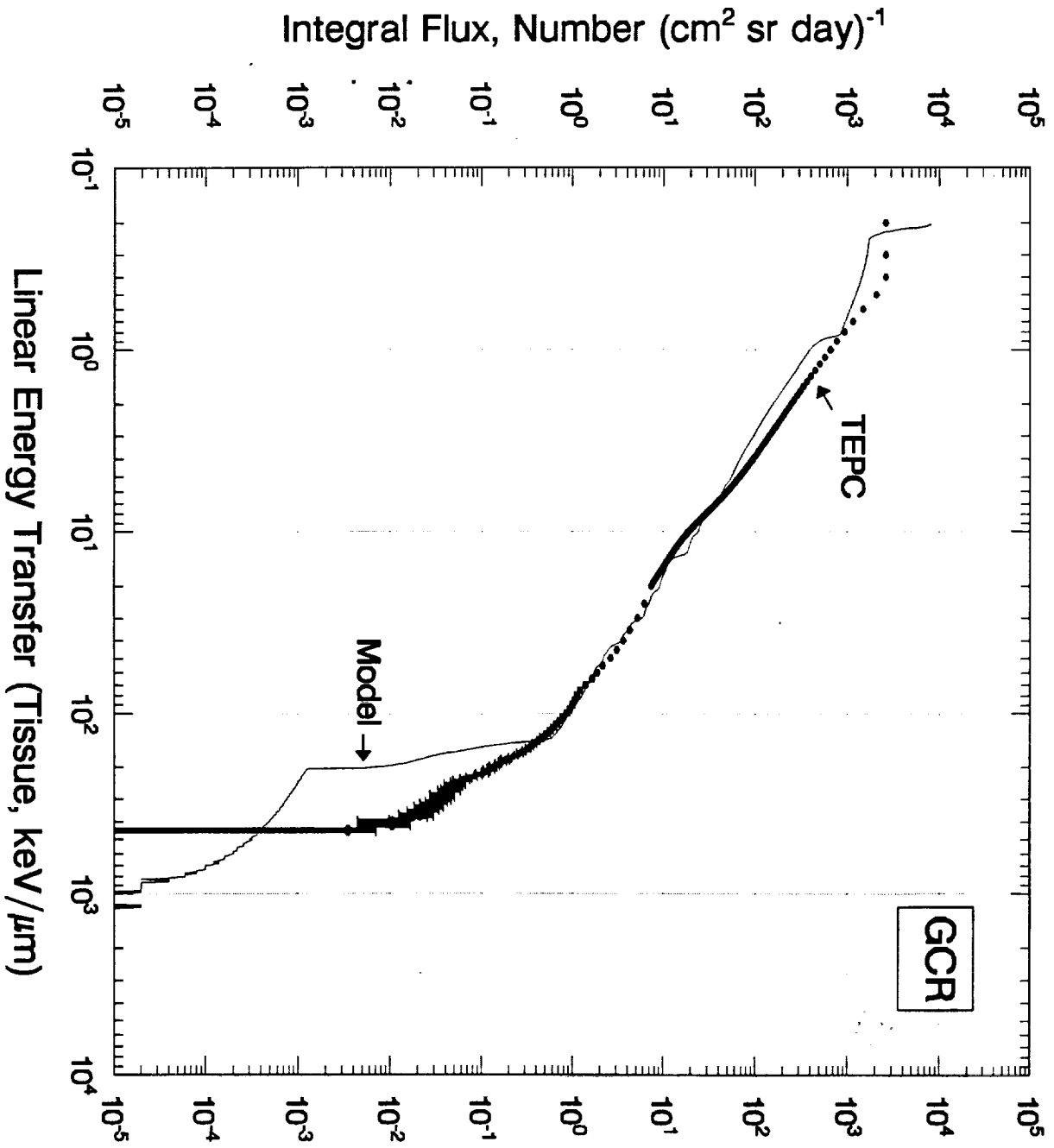


Fig. 7



10/10/2020
10/10/2020
10/10/2020

10/10/2020
10/10/2020